Remote sensing of absorbing aerosols and precipitable water vapor using MFRSR measurements

Mikhail D. Alexandrov[a,b], Brian Cairns[a,b], Andrew A. Lacis[b], Barbara E. Carlson[b]

[a]Department of Applied Physics and Applied Mathematics, Columbia University, New York
[b]NASA Goddard Institute for Space Studies, New York, USA

ABSTRACT

We present further development of our analysis algorithm for Multi-Filter Rotating Shadowband Radiometer (MFRSR) data. The new additions include techniques allowing us to retrieve spectral aerosol single scattering albedo (SSA) and column amount of precipitable water vapor (PWV). The SSA retrievals employ MFRSR measurements of both direct normal and diffuse horizontal irradiances. We present a sensitivity study indicating dependence of SSA retrievals on optical thickness and other aerosol parameters. Influence on the retrievals of a possible error in separation of the direct and diffuse irradiances by the instrument is discussed. The algorithm has been tested on a long-term dataset from the local MFRSR network at the DOE Atmospheric Radiation Measurement (ARM) Program site in Southern Great Plains (SGP). Our results are compared to AERONET's almucantar retrievals of SSA from CIMEL sun-photometer co-located with the MFRSR at the SGP Central Facility. A constrained variant of the algorithm (assuming zero nitrogen dioxide column values) is used for this comparison and to study the influence of the uncertainty associated with this atmospheric gas on the retrieved aerosol absorption properties. Precipitable water vapor column amounts are determined from the direct normal irradiances in the 940 nm MFRSR spectral channel. HITRAN 2004 spectral database has been used to model the water vapor absorption, while a range of other databases (HITRAN 1996, 2000, ESA) is used in the sensitivity study. The results of the PWV retrievals for SGP's MFRSR network are compared with correlative measurements by Microwave Radiometers (MWR), GPS stations, AERONET, and MODIS satellite product. In the latter case an interpolation technique has been used to determine spatial structure of water vapor field from the network data and to create a 2D dataset comparable with satellite data.

Keywords: aerosol absorption, single scattering albedo, precipitable water vapor, aerosol optical thickness, sun-photometry, spatial and temporal variability

1. INTRODUCTION

Atmospheric aerosols and water vapor play important role in Earth's climate system. This role is not limited solely to absorption of solar radiation. Atmospheric aerosols affect the Earths climate also by scattering solar radiation and by altering the lifetime and development of clouds. Water vapor absorbs thermal radiation from the Earth's surface. It is also involved in non-radiative transport (convection and condensation of water) and a number of atmospheric chemical cycles, including those of aerosol formation. Thus, accurate characterization of aerosol properties and water vapor variability using various measurements is needed. Sun-photometric measurements through their high accuracy and good spatial coverage constitute one of the important sources of information on aerosol and water vapor. In this study we present retrieval techniques allowing us to derive aerosol absorption properties and precipitable water vapor (PWV) columns from Multi-Filter Rotating Shadowband Radiometer (MFRSR) data.

The MFRSR[1] makes precise simultaneous measurements of the direct solar beam extinction and horizontal diffuse flux, at six wavelengths (nominally 415, 500, 615, 670, 870, and 940 nm) at short (20 sec in our dataset) intervals throughout the day. Besides water vapor at 940 nm, the other gaseous absorbers within the MFRSR channels are NO_2 (at 415, 500, and 615 nm) and O_3 (at 500, 615, and 670 nm). Aerosols and Rayleigh scattering contribute atmospheric extinction in all MFRSR channels.

Send correspondence to M. Alexandrov: E-mail: malexandrov@giss.nasa.gov

Remote Sensing of Clouds and the Atmosphere XI, edited by James R. Slusser, Klaus Schäfer, Adolfo Comerón,
Proc. of SPIE Vol. 6362, 636202, (2006) · 0277-786X/06/$15 · doi: 10.1117/12.687110

The inversion method[2] allows us to retrieve fine mode and coarse mode aerosol optical thickness (AOT), effective radius of the fine mode, as well as column amounts of ozone and nitrogen dioxide. In this paper we describe the new additions to this algorithm including techniques allowing us to retrieve spectral aerosol single scattering albedo (SSA) and column amount of precipitable water vapor (PWV). The algorithm has been applied to multi-year dataset from the local MFRSR network at the DOE Atmospheric Radiation Measurement (ARM) Program site in Southern Great Plains (SGP). This network consists of 21 instruments (Fig. 3, left) located at SGP's Extended Facilities (EFs) and covers the area of approximately 3 by 4 degrees in northern Oklahoma and southern Kansas with average spacing of 80 km between neighboring measurement sites. The SGP's Central Facility (CF) contains two co-located MFRSRs (C1, E13), which can be compared to check for retrieval consistency. A number of different sensors deployed at SGP's CF (AERONET's CIMEL sun-photometer, Microwave Radiometer, GPS system, lidars, etc.) provide a unique opportunity to validate and enhance MFRSR retrievals through intercomparisons with other measurements.

2. RETRIVAL OF AEROSOL ABSORPTION PROPERTIES

The diffuse component of downwelling solar irradiance can be used for determination of aerosol absorption properties, such as imaginary part of refractive index and single scattering albedo (SSA).[3–5] Given the retrieved aerosol optical thickness and size information, we can calculate the diffuse transmission for a specific refractive index to compare with the measured diffuse irradiance. We actually use the ratios between the direct and diffuse irradiances (direct/diffuse ratios) in our retrieval algorithm. We use a plane-parallel scalar adding-doubling code to compute a look-up table of diffuse transmission functions depending on solar zenith angle, AOT at 870 nm, fine mode fraction in 870 nm AOT, fine mode effective radius, NO_2 column amount, and the imaginary part of refractive index. A separate table for SSA depending on the above parameters is also computed. Rayleigh scattering is accounted for in the radiative transfer model, while ozone absorption was not taken into account, since the overwhelming part of ozone is located above the aerosol layer, thus, its absorption tends to cancel out in the direct-diffuse ratio (off-line tests support this conclusion). The values of aerosol parameters (and NO_2 column in unconstrained algorithm) are derived using our previously published method.[2] Surface albedos used in computations were taken from two-year MODIS composite product (A. Trishchenko, *private communication*).

Estimated values of aerosol spectral SSA retrieved from both SGPs Central Facility MFRSRs (C1 and E13) are shown in Fig. 1(top panels) as plots of time series of daily means for September 2000. The correlative values of SSA obtained through AERONETs almucantar scan analysis[6] are shown for comparison. The AERONET's CIMEL sun-photometer (Cart Site) is co-located with the two MFRSRs at the Central Facility. The SSA retrievals shown are for 500 and 870 nm channels common for MFRSR and CIMEL sunphotometers, although the retrievals have been made for all MFRSR channels except 940 nm affected by water vapor absorption (see below). The constrained version[2,7] of the retrieval algorithm neglecting NO_2 absorption is used in this study since AERONET retrievals are made with the same assumption. While NO_2 absorption does not significantly affect SSA retrievals at 500 nm and longer wavelengths, its influence on SSA in 415 nm channel can be significant causing retrieval error up to 0.05 (for the dataset presented). It has been also reported[8] that neglect of absorption of 2 DU of NO_2 in UV region (368 nm) can result in underestimation of aerosol SSA by as much as 0.1.

The large differences in retrieved SSA (Fig, 1, top panels) between MFRSRs and CIMEL suggest that MFRSR measurements underestimate the diffuse irradiance, particularly during the last half of September 2000. During this period AOT was relatively low (lower than 0.2 at 500 nm, Fig. 2, top left panel) and the diffuse irradiance was also low compared to the direct beam (by a factor greater than 4 at 500 nm, Fig. 2, top right panel). The bottom panels of Fig. 2 indicate that small AOT in the last half of September 2000 also corresponds to smaller fraction of fine mode in total optical thickness ($\tau_{\text{fine}}/\tau_{\text{total}}$), and, therefore, to larger effective particle size. It is clear, that the smaller the amount of aerosol studied, the greater uncertainty in its retrieved properties one may expect. Note, that AERONET does not provide retrievals for particularly low AOTs, and the recommended minimal AOT for SSA retrievals is 0.4 at 440 nm. On the other hand, the observed correlation between SSA and AOT may have a physical explanation[9]: "... pollution coming from combustion sources such as industry and mobile sources, after some aging, forms the background aerosol, which contains sufficient soot to give the high absorption number. Once other particles are added ... or water due to high humidity, the scattering coefficient

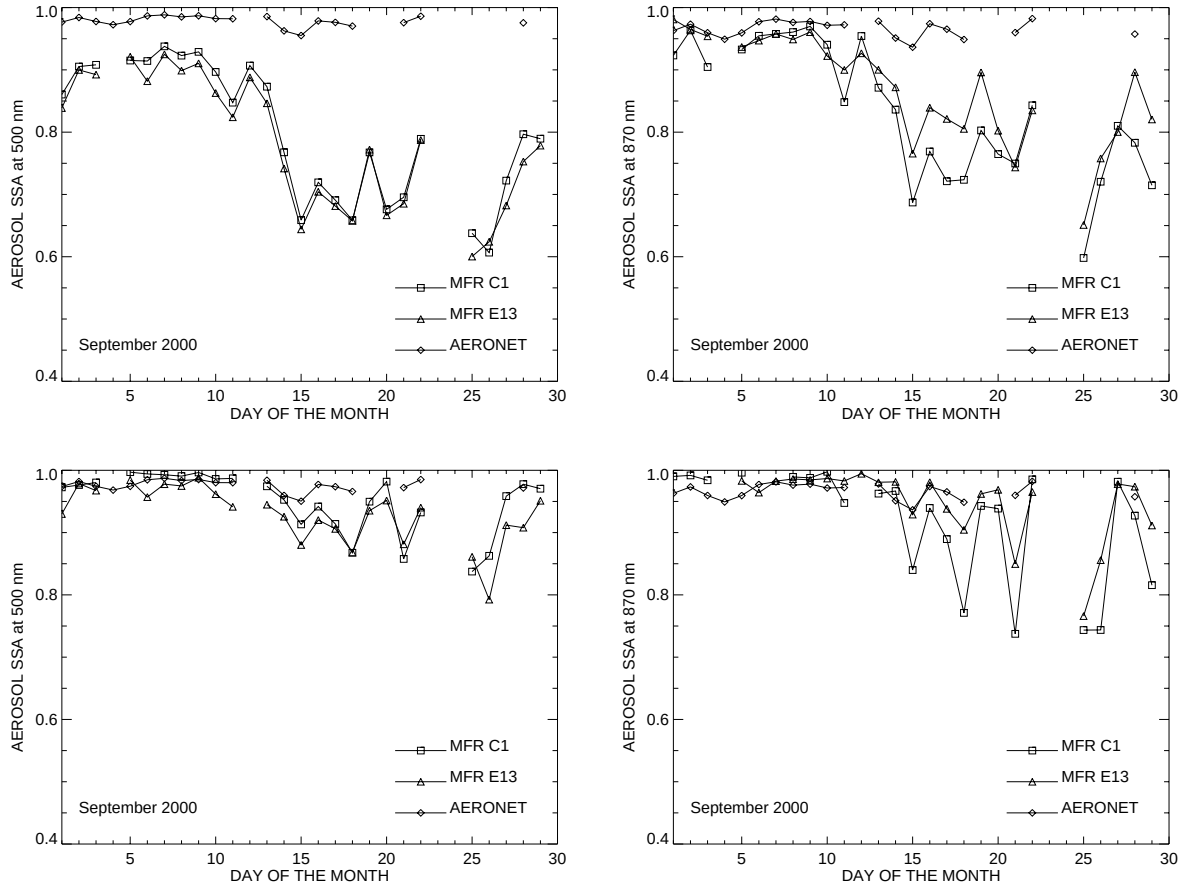

Figure 1. Top: time series of daily mean values of aerosol SSA (in 500 and 870 nm channels) retrieved from measurements by SGP Central Facility MFRSRs (C1, E13) made in September 2000 (preliminary results). Correlative AERONETs values from almucantar scan analysis are shown for comparison. Constrained (zero NO_2) MFRSR analysis algorithm had been used for these plots. Bottom: SSA retrievals for the same period made with empirical correction of separation between direct and diffuse irradiances.

increases, while the absorption coefficient remains almost the same". However, the values of SSA lower than 0.8 still look suspicious, especially in comparison with much higher AERONET's numbers.

The above discrepancy in SSA retrievals could be caused by an imperfect separation between direct and diffuse irradiances by the MFRSR shadowbanding technique[1] using two side (9^o off-sun) block measurements to correct for the part of the solar aureole entering the measurement of the direct beam. This separation error creates a bias in the measured diffuse flux due to the solar aureole not being fully credited to the diffuse irradiance and results in subtracting out some fraction δ of the diffuse irradiance and counting it as part of the direct beam. This bias would be more severe for larger and/or more absorbing aerosol particles which have a narrower aureole, and would also be a function of wavelength and viewing geometry. To obtain a more quantitative estimate of the direct/diffuse separation bias we developed an empirical correction to the direct/diffuse ratios as follows. With the original direct/diffuse ratio defined as

$$D = \frac{I_{\rm dir}}{I_{\rm dif}}, \tag{1}$$

the modified ratio

$$D' = \frac{I_{\rm dir} - \delta \cdot I_{\rm dif}/\cos(\theta)}{(1+\delta) \cdot I_{\rm dif}}, \tag{2}$$

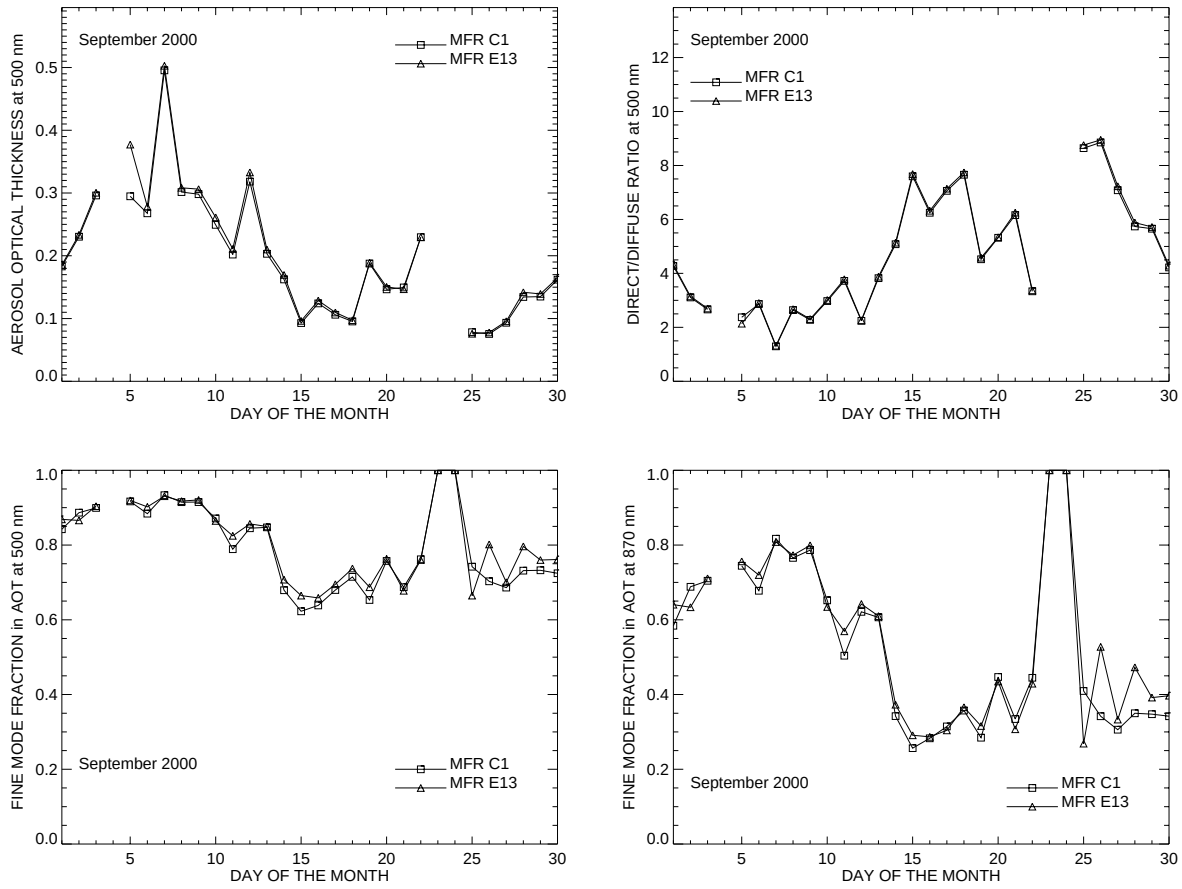

Figure 2. Time series for september 2000 of daily mean aerosol optical thickness in 500 nm channel (top left), the ratio between direct normal and diffuse horizontal irradiances (top right), and the fine mode fractions in 500 and 870 nm AOT (bottom).

implies transfer of a part of irradiance from direct into diffuse (here θ is the solar zenith angle). Since a portion δ of irradiance to be transferred should depend on aerosol particle size due to its influence on the width of solar aureole, we define

$$\delta = 0.2 \cdot \left(1 - \frac{\tau_{\text{fine}}(870\text{nm})}{\tau_{\text{total}}(870\text{nm})}\right). \tag{3}$$

While this correction is not precise, it is sufficient to indicate the sensitivity of SSA retrievals to separation of direct and diffuse irradiances. Comparison between top and bottom panels of Fig. 1 shows notable increase in the retrieved SSA values after the correction (2) is applied. It has been also observed (E. Kassianov, *private communication*), that treatment of MFRSR data as these from a tracking radiometer implying "field of view" correction for the portion of forward-scattered diffuse radiation registered as direct by the instrument can significantly increase low SSA retrievals (e.g. from 0.6 to 0.8). However, there remain spikes of SSA in Fig. 1(bottom) that are lower than 0.8 that appear to be associated with low AOT and low fine mode fraction (Fig. 2), situations that would exacerbate the direct/diffuse bias. Clearly, the angular distribution of the diffuse radiance field becomes less uniform at low aerosol loading and in the presence of absorption and larger aerosol particles. This suggests the need for a rigorous sensitivity study involving actual modeling of shadowband operation necessary to estimate (and possibly correct for) the actual shadowbanding error under various atmospheric conditions.

Another anomaly seen in the uncorrected SSA retrievals is the inversion in the spectral dependence of SSA:

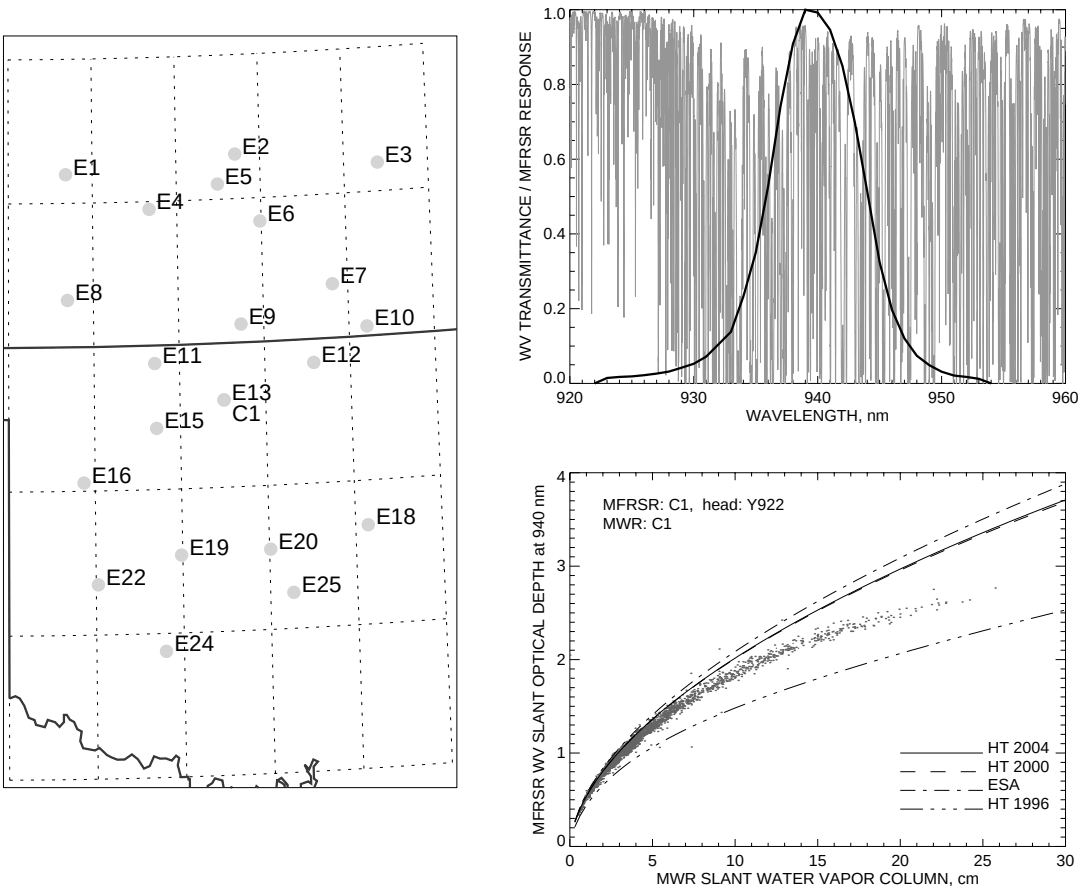

Figure 3. Left: Locations of MFRSRs at the DOE ARM program CART site in the Southern Great Plains (SGP). The location of the Extended Facility E13 coincides with the Central Facility C1. Right top: Spectral transmittance of PWV corresponding to 1 cm column computed using HITRAN 2004 database (grey), and the MFRSR (head 922) 940 nm channel spectral response function normalized to unity at the maximum (black). Right bottom: Experimental growth curve constructed by plotting MFRSR-derived slant optical thickness in 940 nm channel (with AOT and Rayleygh subtracted) v.s. MWR-derived slant PWV column (SGP CF, 2000). The growth curves obtained by integrating MFRSR spectral response functions with WV absorption spectra from various databases (HITRAN 1996, 2000, 2004, European Space Agency (ESA)) are shown by lines.

while its values decrease with wavelength in first four channels, the SSA in 870 nm channel is greater than this in 670 nm channel, and even in 500 nm channel. This may be caused by the difference (e.g. due to variation in vegetation parameters) between actual spectral surface reflectances and the model values used in the retrievals. We continue to work on improvement of our SSA retrievals and on detection of possible instrumental problems, which may affect them.

3. RETRIEVAL OF PRECIPITABLE WATER VAPOR COLUMN

Sun-photometric measurements of direct normal irradiances in 940 nm channel can be used for retrieval of Precipitable Water Vapor (PWV) column.[10–12] Our retrieval method for MFRSR data is based on inversion of

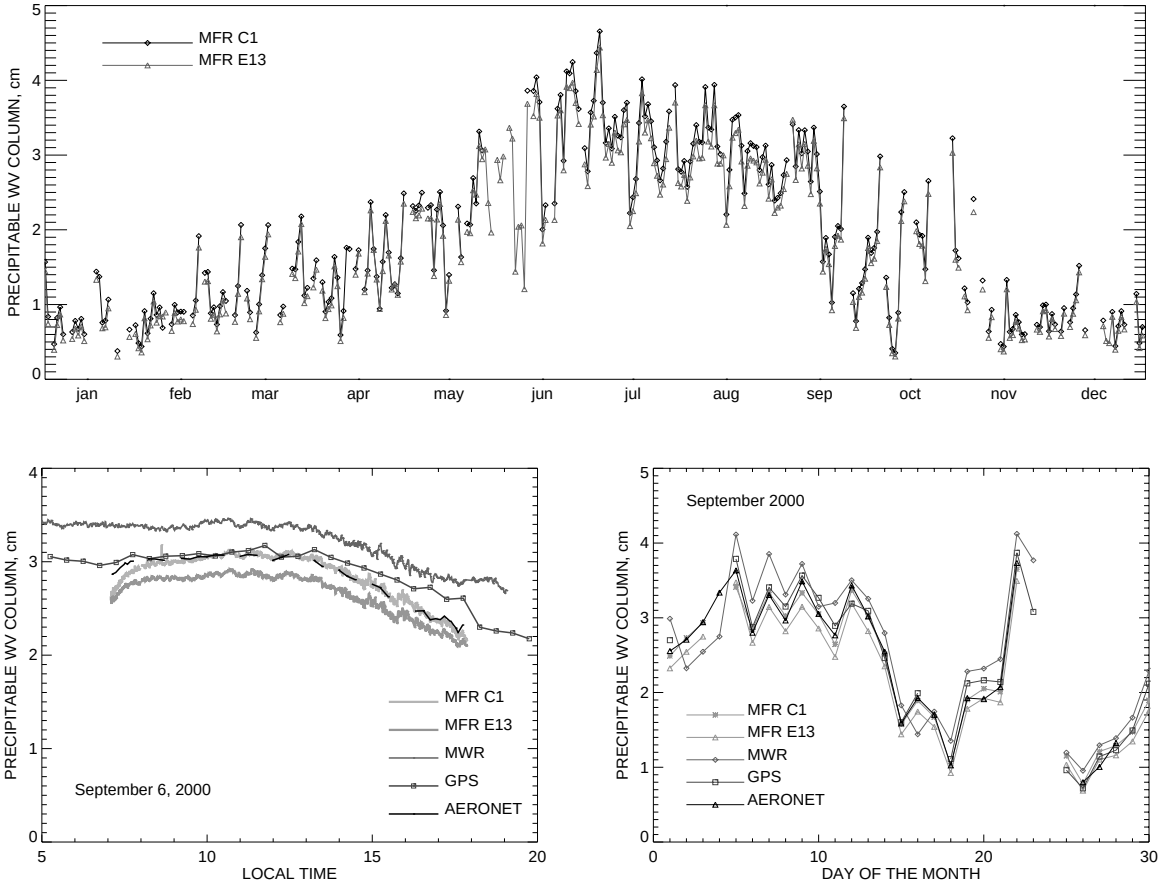

Figure 4. Top: Retrievals of column PWV for the year 2000 data from the two MFRSRs at SGPs Central Facility (C1 and E13). Bottom: Comparison of the MFRSR PWV retrievals with the correlative data from MWR, GPS, and AERONET for a single day (Sept. 6, left) for the whole month of September 2000 (daily mean values, right). C1 data appears to be almost indistinguishable from AERONET retrievals and in better agreement with GPS than with MWR, which yields systematically higher values.

the curve of growth relating the 940 nm slant optical depth of PWV

$$\tau_w^{(sl)} = m\ \tau_w = m\ (\tau - \tau_r - \tau_a) \tag{4}$$

and the slant PWV column

$$u^{(sl)} = m\ u. \tag{5}$$

Here u is the vertical PWV column, m is the airmass depending on solar zenith angle, τ is the total optical thickness in 940 nm channel, τ_w is the (vertical) optical thickness of PWV, τ_R is the Rayleigh optical thickness,[13] τ_a is the aerosol optical thickness determined using Mie theory applied to the aerosol parameters derived[2] from the data in the first five MFRSR channels. The growth curve for a particular instrument is computed by integration over wavelength λ of PWV spectral transmittance $T_w(\lambda, u^{(sl)})$ (computed using a spectral database, e.g. HITRAN, for a standard atmospheric profile) with the laboratory-measured spectral response function $f(\lambda)$

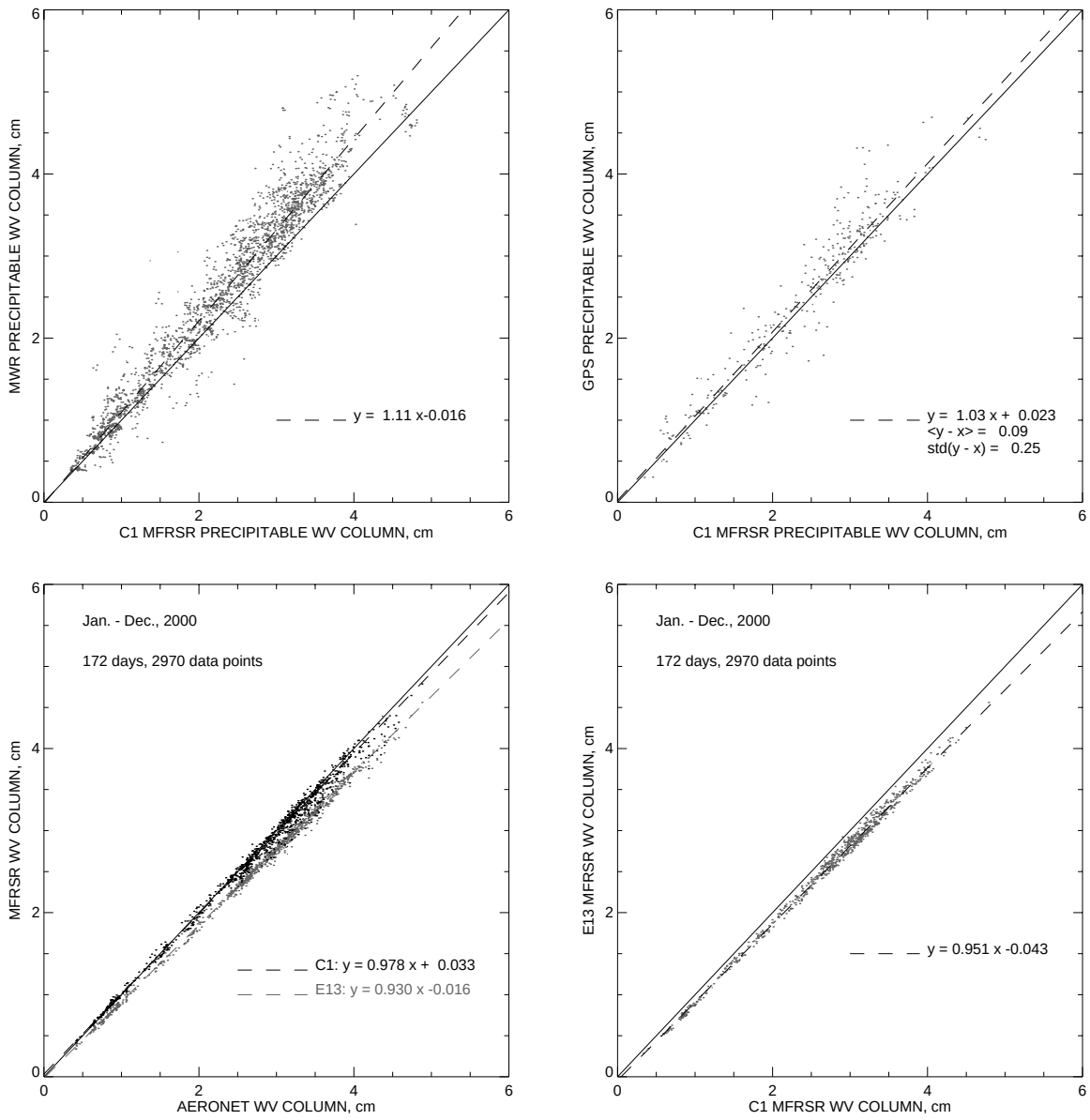

Figure 5. Comparison between column PWV retrievals from C1 MFRSR and those from co-located MWR (C1, top left) and Wind Profiler Demo Network (WPDN) GPS station (top right). While MWR values show 11% bias relaive to C1 MFRSR, GPS results are in better agreement with C1 (3% bias). Bottom left: Comparison between column PWV retrievals from C1 and E13 MFRSRs and those from co-located AERONETs CIMEL sun-photometer ("Cart Site"). AERONET results show only 2% bias relative to C1 MFRSR. The difference in retrievals between the two MFRSRs (bottom right) is probably due to errors in spectral response characterizations of the instruments 940 nm channels.

of the 940 nm channel of this instrument. The integration is weighted with the TOA solar irradiance $I_0(\lambda)$:

$$\tau_w^{(sl)}(u^{(sl)}) = -\ln\left[\frac{\int_{\lambda_1}^{\lambda_2} T_w(\lambda, u^{(sl)}) f(\lambda) I_0(\lambda)\ \mathrm{d}\lambda}{\int_{\lambda_1}^{\lambda_2} f(\lambda) I_0(\lambda)\ \mathrm{d}\lambda}\right]. \tag{6}$$

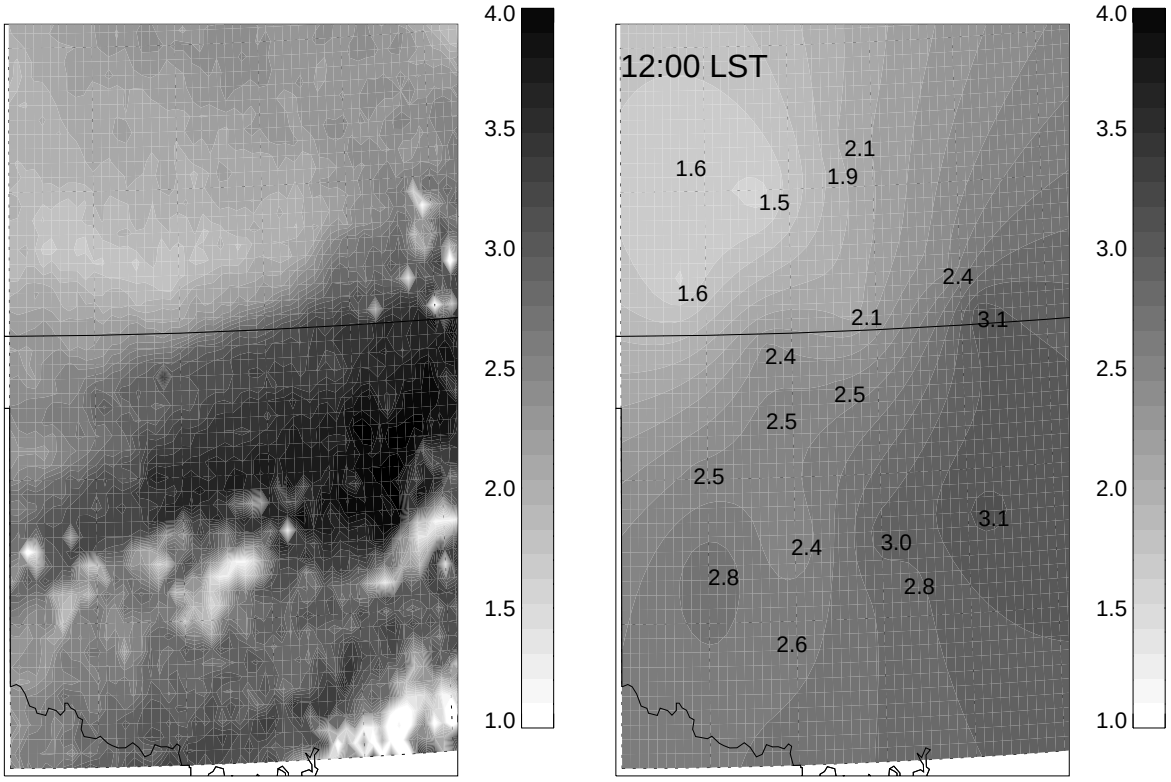

Figure 6. MODIS Level 2 WV product over SGP site (left) and spatial structure obtained by interpolation of MFRSR network data (left) from 12:00 noon on September 14, 2000. The numbers show the PWV column values (in cm) for each MFRSR location.

The growth curve can usually be represented as a power law function ($\tau_w^{(sl)} \approx a(mu)^b$, with $b \approx 0.6$ and a as adjustable parameters). This paprametrization, however, is not very accurate at large airmasses,[12] so we use the actual growth curve in our inversions. The power-law parameterization is useful in the "modified Langley plot" calibration technique,[14, 15] which can provide very approximate characterization due to high variability of PWV column amounts. In our data analysis we rely on laboratory calibration of 940 nm MFRSR channel.

An example of $f(\lambda)$ (normalized to unity at responses maximum) is given in Fig. 3(right top) for the MFRSR head 922 installed on C1 instrument during the year 2000. The spectral response function is plotted over the spectral transmittance of PWV corresponding to 1 cm column and computed using HITRAN 2004 database. While the instrument response functions are not always accurately determined, the main problem affecting the PWV retrievals in the recent years has been related to uncertainties in spectral databases of water vapor absorption. These uncertainties are illustrated in Fig. 3(right bottom) by comparing of the growth curves computed for MFRSR's head 922 using four different spectral databases: HITRAN 96, 2000, 2004 (http://cfa-www.harvard.edu/hitran/) and European Space Agency (ESA) database (http://www.sstd.rl.ac.uk/sg/Data/Esa-wv/). These curves differ quite significantly one from each other and from the experimental curve obtained by plotting MFRSR-derived slant optical thickness at 940 nm (with AOT and Rayleigh contribution subtracted) v.s. PWV slant column derived from co-located Microwave Radiometer (MWR) measurements. However, the two most recent databases, HITRAN 2000 and 2004, yield almost identical results suggesting that perhaps the spectral databases are converging, and HITRAN 2004[16] is suitable for long-term multi-site retrievals.

We performed retrievals of PWV column amounts for the data from all SGPs Extended Facilities for the year 2000. Figure 4 shows these retrievals for the Central Facility MFRSRs (C1, E13). A strong summer maximum in

PWV column is clearly seen. The MFRSR retrievals are compared in Fig. 4(bottom) with the correlative data from Microwave Radiometer (MWR, C1), Global Positional System (GPS) station from Wind Profiler Demo Network (WPDN), and AERONET (Cart Site location). The comparisons are shown for a one day (Sept. 6, 2000) instantaneous data and for the month-long (September 2000) time series of daily mean values.

The systematic 5% difference between the values from co-located C1 and E13 MFRSRS observed in Fig. 4 and seen more clearly in Fig. 5(bottom right) is likely due to uncertainties in the laboratory-measured spectral responses of their 940 nm filters. Comparisons presented in Fig. 5 show that C1 MFRSR retrievals are very close to AERONET's values (2% bias) and in better agreement with GPS (3% bias) than with MWR (11% bias). MWR yields systematically higher values then other instruments. Given high temporal variability of PWV column, this level of disagreement may be acceptable, since the measurement uncertainty does not exceed sampling error due to the choice of measurement time.

Spatial density of SGP MFRSR network allows us to reliably interpolate between PWV values obtained at the measurement locations to produce an estimate of PWV spatial distribution over the area. Figure 6(right) shows such a spatial distribution constructed from the MFRSR data obtained on September 14, 2000 at noon (overpass time of Terra satellite). This distribution is in qualitative agreement with corresponding map representing from Terra MODIS PWV product (Fig. 6(left)). While lacking small-scale details (some of which are due to presence of clouds in MODIS image), the MFRSR network provides an accurate spatial trend of PWV: increase from north-west to south-east of the site (note the cloud contamination in the southern part of the MODIS image). The spatial and temporal structures of MFRSR and MODIS datasets for SGP area are complementary to each other: while MODIS provides high spatial resolution at a single time moment for a given day, MFRSRs measurements, though being spatially more sparse, are made continuously in time. This opens an opportunity for future data fusion between the two datasets.

4. DISCUSSION

We presented new additions to our analysis algorithm for MFRSR data, including techniques allowing us to retrieve spectral aerosol single scattering albedo and column amount of precipitable water vapor. The algorithm has been tested on a long-term dataset from the local MFRSR network at the DOE Atmospheric Radiation Measurement (ARM) Program site in Southern Great Plains (SGP). Retrieval results for the year 2000 are presented.

The SSA retrievals from MFRSR data are based on consistency between the measurements of direct normal and diffuse horizontal irradiances. Our results are compared to AERONET's almucantar retrievals of SSA from CIMEL sun-photometer co-located with the MFRSR at the SGP Central Facility. A constrained variant of the algorithm (assuming zero nitrogen dioxide column values) is used for this comparison and to study the influence of the uncertainty associated with this atmospheric gas on the retrieved aerosol absorption properties. The sensitivity study presented in Figs. 1 and 2 indicates that SSA retrievals from MFRSR are biased probably due to instrument error in separation of the direct and diffuse irradiances. We demonstrated, that the retrieval results may be significantly improved if a physically justified correction is applied to the measured direct/diffuse ratios. This correction would be similar to the field of view correction for tracking sun-photometers. Development of such correction would involve detailed modelling of the shadowbanding process and is a part of our future work.

Precipitable water vapor column amounts are determined from the direct normal irradiances in the 940 nm MFRSR spectral channel. We used HITRAN 2004 spectral database to model the water vapor absorption, while other databases (HITRAN 1996, 2000, ESA) have been used in sensitivity study (Fig. 3). The results of the PWV retrievals for SGP's MFRSR network were compared with correlative measurements by Microwave Radiometers (MWR), GPS stations, AERONET, and MODIS satellite product. In the latter case an interpolation technique has been used to determine spatial structure of water vapor field from the network data and to create a 2D dataset comparable with satellite images.

ACKNOWLEDGMENTS

We would like to thank E. Kassianov, A. Trishchenko, J. Liljegren, and A. Smirnov for useful discussions. We thank Rick Wagener for his effort in maintaining the AERONET site at SGP. This research was supported

by the Atmospheric Radiation Measurement (ARM) Program sponsored by the U.S. Department of Energy, Office of Science, Office of Biological and Environmental Research, Environmental Sciences Division (Interagency Agreements No. DE-AI02-93ER61744 and DE-AI02-95ER61961), and by NASA's Radiation Science Program (RTOP No. 622-46-05-30).

REFERENCES

1. L. Harrison, J. Michalsky, and J. Berndt, "Automated multifilter shadow-band radiometer: instrument for optical depth and radiation measurement," *Appl. Opt.* **33**, pp. 5118–5125, 1994.
2. M. Alexandrov, B. Carlson, A. Lacis, and B. Cairns, "Separation of fine and coarse aerosol modes in MFRSR data sets," *J. Geophys. Res.* **110**, D13204, doi:10.1029/2004JD005226, 2005.
3. M. D. King and B. M. Herman, "Determination of the ground albedo and the index of absorption of atmospheric particulates by remote sensing. part i: theory," *J. Atmos. Sci.* **36**, pp. 163–173, 1979.
4. M. D. King, "Determination of the ground albedo and the index of absorption of atmospheric particulates by remote sensing. Part II: application," *J. Atmos. Sci.* **36**, pp. 1072–1083, 1979.
5. E. I. Kassianov, J. C. Barnard, and T. P. Ackerman, "Retrieval of aerosol microphysical properties using surface MultiFilter Rotating Shadowband Radiometer (MFRSR) data: Modeling and observations," *J. Geophys. Res.* **110**, p. doi:10.1029/2004JD005337, 2005.
6. O. Dubovik and M. D. King, "A flexible inversion algorithm for retrieval of aerosol optical properties from Sun and sky radiance measurements," *J. Geophys. Res.* **105**, pp. 20673–20696, 2000.
7. M. Alexandrov, B. Carlson, A. Lacis, and B. Cairns, "Remote sensing of fine and coarse mode atmospheric aerosols using ground-based sun-photometry," in *Remote Sensing of Clouds and Atmosphere X*, K. Schäfer, A. Comeron, J. R. Slusser, R. H. Picard, M. R. Carleer, and N. I. Sifakis, eds., *Proc. SPIE* **5979**, p. 59790L, 2005.
8. A. Cede, J. Herman, A. Richter, N. Krotkov, and J. Burrows, "Measurements of nitrogen dioxide total column amounts using a Brewer double spectrometer in direct Sun mode," *J. Geophys. Res.* **111**, pp. D05304, doi:10.1029/2005JD006585, 2006.
9. H. Horvath, L. A. Arboledas, F. J. Olmo, O. Jovanovic, M. Gangl, W. Kaller, C. Sanchez, H. Sauerzopf, and S. Seidl, "Optical characteristics of the aerosol in spain and austria and its effect on radiative forcing," *J. Geophys. Res.* **107**, p. doi:10.1029/2001JD001472, 2002.
10. J. J. Michalsky, J. C. Liljegren, and L. C. Harrison, "A comparison of sunphotometer derivations of total column water vapor and ozone to standard measures of same at the Southern Great Plains atmospheric radiation measurement site," *J. Geophys. Res.* **100**, pp. 25995–26003, 1995.
11. T. Ingold, B. Schmid, C. Matzler, P. Demoulin, and N. Kampfer, "Modeled and empirical approaches for retrieving columnar water vapor from solar transmittance measurements in the 0.72, 0.82, and 0.94 μm absorption bands," *J. Geophys. Res.* **105**, pp. 24327–24343, 2000.
12. B. Schmid, J. J. Michalsky, D. W. Slater, J. C. Barnard, R. N. Halthore, J. C. Liljegren, B. N. Holben, T. F. Eck, J. M. Livingston, P. B. Russel, T. Ingold, and I. Slutsker, "Comparison of columnar water-vapor measurements from solar transmittance methods," *App. Opt.* **40**, pp. 1886–1896, 2001.
13. J. E. Hansen and L. D. Travis, "Light scattering in planetary atmospheres," *Space Sci. Rev.* **16**, pp. 527–610, 1974.
14. J. Reagan, K. Thome, B. Herman, and R. Gall, "Water vapor measurements in the 0.94 micron absorption band: Calibration, measurements, and data applications," *Proc. Int. Geoscience and Remote Sensing '87 Symposium, Ann Arbor, Michigan, IEEE* , pp. 63–67, 1987.
15. J. A. Reagan, P. A. Pilewskie, I. C. Scott-Fleming, B. M. Herman, and A. Ben-David, "Extrapolation of Earth-based solar irradiance measurements to exoatmospheric levels for broad-band and selected absorption-band observations," *IEEE Geosc. Rem. Sens.* **25**, pp. 647–653, 1987.
16. L. S. Rothman, D. Jacquemart, A. Barbe, D. C. Benner, M. Birk, L. R. Brown, M. R. Carleer, C. C. Jr., K. Chance, L. H. Coudert, V. Dana, V. M. Devi, J.-M. Flaud, R. R. Gamache, A. Goldman, J.-M. Hartmann, K. W. Jucks, A. G. Maki, J.-Y. Mandin, S. T. Massien, J. Orphal, A. Perrin, C. P. Rinsland, M. A. H. Smith, J. Tennyson, R. N. Tolchenov, R. A. Toth, J. V. Auwera, P. Varanasi, and G. Wagner, "The HITRAN 2004 molecular spectroscopic database," *JQSRT* **96**, pp. 139–204, 2005.